d-d Excitations in Manganites Probed by Resonant Inelastic X-Ray Scattering

S. Grenier,[1,2] J. P. Hill,[2] V. Kiryukhin,[1] W. Ku,[2] Y.-J. Kim,[2] K. J. Thomas,[2] S-W. Cheong,[1] Y. Tokura,[3] Y. Tomioka,[3] D. Casa,[4] and T. Gog[4]

[1]*Department of Physics and Astronomy, Rutgers University, Piscataway, New Jersey 08854, USA*
[2]*Department of Physics, Brookhaven National Laboratory, Upton, New York 11973, USA*
[3]*Joint Research Center for Atom Technology (JRCAT), Tsukuba 305-0046, Japan*
[4]*CMC-CAT, Advanced Photon Source, Argonne National Laboratory, Argonne, Illinois 60439, USA*

(Received 9 July 2004; published 3 February 2005)

We report a study of electronic excitations in manganites exhibiting a range of ground states, using resonant inelastic x-ray scattering (RIXS) at the Mn *K* edge. Excitations with temperature dependent changes correlated with the magnetism were observed as high as 10 eV. By calculating Wannier functions, and finite-*q* response functions, we associate this dependence with intersite *d-d* excitations. The calculated dynamical structure factor is found to be similar to the RIXS spectra.

DOI: 10.1103/PhysRevLett.94.047203 PACS numbers: 75.47.Lx, 61.10.–i, 71.27.+a, 74.25.Jb

The diverse range of magnetic and electronic ground states exhibited by manganites arises from cooperative and competing interactions involving the spin, orbital, and charge degrees of freedom and electron-lattice coupling. A complete understanding of the relative importance of these interactions, as well as an interpretation of many experimental observations remain lacking [1,2]. Theoretical approaches typically integrate out the oxygen degrees of freedom and parametrize the behavior of the Mn $3d$ orbitals with terms such as the hopping amplitude between neighboring Mn sites, the on-site Coulomb repulsion (U), and the Hund's coupling (J), each of which are on the order of several eV. Measurements of the excitation spectra up to these energies can thus play a key role in the understanding of these systems, providing a more stringent test of a given model than do ground state measurements. Central to such efforts will be understanding how the excitations relate to the various ground states.

In this Letter, we report the electronic excitation spectra for a range of manganite ground states using resonant inelastic x-ray scattering (RIXS). Significantly, our results show systematic temperature dependencies that are associated with magnetic ordering at energy scales up to 10 eV: The integrated spectral weight in the $1 \rightarrow 5$ eV energy range increases (decreases) on entering a ferromagnetic (antiferromagnetic) phase and is unchanged through metal-insulator transitions—if the magnetic ground state is unchanged. We calculate the RIXS response function of the parent $LaMnO_3$ utilizing time-dependent density functional theory. The electronic structure and the spatial distributions of the ordered orbitals are obtained, showing the orbital ordering and that the Mn highest occupied and lowest unoccupied states stretch to the first (O) and second neighbors (Mn). On the basis of these calculations, the temperature dependence is found to arise from intersite *d-d* excitations mediated by the oxygen hybridization. These excitations are enhanced (suppressed) by nearest neighbors ferromagnetic (antiferromagnetic) correlations.

Inelastic x-ray scattering (IXS) is a photon in/photon out probe of electronic excitations over energy scales up to and above the charge-transfer gap, capable of covering the entire Brillouin zone with bulk sensitivity. By tuning the photon energy to the absorption edge (or ''resonance''), the IXS cross section is enhanced, allowing even high-Z based systems to be studied [3,4], albeit at the price of a more complicated cross section.

In the present work, samples with several magnetic, orbital, charge, and structural ground states were studied: $La_{0.875}Sr_{0.125}MnO_3$ (hereafter referred to as LSMO.125), which has a paramagnetic semiconductor (PMSC) to ferromagnetic metal (FM) phase transition at 190 K and is a ferromagnetic insulator (FI) below 150 K; $La_{0.7}Ca_{0.3}MnO_3$ (LCMO.3), which is a PMSC above $T_C = 250$ K and FM below; $Pr_{0.6}Ca_{0.4}MnO_3$ (PCMO.4), which undergoes a phase transition from PMSC to a two-dimensional antiferromagnetic insulator (AFI) at 234 K with the onset of orbital ordering, and becomes AFI at $T_N = 180$ K; and $Nd_{0.5}Sr_{0.5}MnO_3$ (NSMO.5), which has a PMSC to FM transition at 250 K, and a FM to orbitally ordered AFI transition at 150 K. All samples were grown by the floating zone method. Their quality was checked by x-ray diffraction, resistivity, and magnetization measurements.

The experiments were performed at beam line 9IDB (CMC-CAT, Advanced Photon Source). We used Si(111) and Si(311) monochromators and a spherically bent Ge(531) analyzer that focuses the scattered x rays onto a solid-state detector. The overall resolution was 300 meV (FWHM). The incident photons were linearly polarized, perpendicular to the scattering plane. The incident energy (E_i) was tuned to the peak of the Mn *K*-edge absorption of the respective materials for which the RIXS intensity was maximized. The inelastic scattering arises from the recombination of the exciton comprised of the $1s$ core hole and the $4p$ photoelectron, after it has exchanged energy with the valence electrons. The data were taken at a fixed $Q = (0\ 2.3\ 0)$ to minimize elastic scattering from the Bragg

reflections (0 2 0)- and (0 2.5 0)-*Pbnm* settings. Here and in other studies, little or no Q dispersion was observed in contrast to the case for cuprates [5–8].

Representative spectra for LSMO.125 are shown in Fig. 1. Data were taken on cooling from a paramagnetic semiconducting phase into a ferromagnetic phase. Remarkably, temperature dependence is observed up to 10 eV. The spectra are characterized by three distinct regions: the region up to 6 eV, which shows an increase on cooling into the ferromagnetic phase; a region between 6 and 10 eV with opposite temperature dependence; and a peak at around 12 eV with no systematic temperature dependence. In what follows, we will focus primarily on the lowest energy region.

To do so quantitatively, we must first subtract the elastic scattering, which increases with temperature as a result of quasielastic scattering from phonons. This was carried out by assuming that the elastic line is symmetric and by subtracting the energy-gain side from the energy-loss side. This assumption was shown to be valid by measuring the elastic scattering off resonance (Fig. 1). We believe this procedure gives reliable spectra above 1.5 eV. The results for the four samples are shown in the left panels of Fig. 2.

In all samples, the lowest energy feature in the subtracted spectra occurs around ~2 eV; i.e., at 2.75 ± 0.1 eV for LSMO.125, at 2.6 ± 0.1 eV for LCMO.3, at 1.9 ± 0.1 eV for PCMO.4, and at 2.0 ± 0.1 eV for NSMO.5. This "2 eV" feature is reminiscent of the one observed in optical conductivity studies [10–14]. Note that there is an apparent trend in this feature to move to lower energies with higher doping. Inami *et al.* reported a similar feature at 2.5 ± 0.25 eV in $LaMnO_3$ [5], which fits into this same trend. The data for PCMO.4 show that this feature is still present on warming through the orbital ordering transition ($T_{OO} = 234$ K) and that therefore this feature cannot be associated with long-range orbital order. Our data suggest that some contribution of the spectral weight about 2 eV is temperature independent; see, in particular, the NSMO.5 data where the temperature dependence clearly occurs at higher energies, about 3.25 eV. This suggests that the low-energy spectrum corresponds to at least two processes. These could be d-d (T dependent) and $2p$-d charge transfer (T independent), which have both been proposed and are not exclusive [14–17]. We focus in the following on the temperature dependence.

In order to characterize the low-energy spectra in a model-independent way, we have summed the intensity between 1.5 and 5 eV (right panels of Fig. 2). These panels illustrate the central result, namely, that the integrated spectral weight follows the magnetization of the sample in a systematic way, and that this result is independent of the conductivity of the ground state.

Specifically, for LSMO.125, LCMO.3, and NSMO.5 the integrated intensity increases on cooling into a ferromagnetic metallic phase. Conversely, the intensity clearly drops on entering an antiferromagnetic phase (PCMO.4 and NSMO.5). Finally, in LSMO.125 ($T_{MI} = 150$ K), there is a smooth increase in intensity as this sample is cooled through T_{MI} into the ferromagnetic insulating phase. Thus, we conclude that the change in the inelastic scattering reflects the magnetic order, not the electrical conductivity. The exact relationship between the RIXS

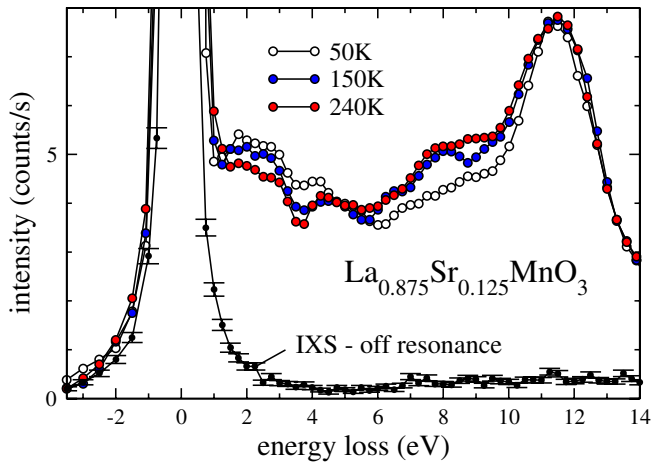

FIG. 1 (color online). Energy loss spectra of LSMO.125 versus temperature. Each point is averaged over three consecutive data points to decrease the statistical noise. The elastic line (0 eV) was typically 1000 counts/s. Error bars are typically 0.15 counts/s. An off-resonance spectrum is also shown ($E_i = 6538$ eV).

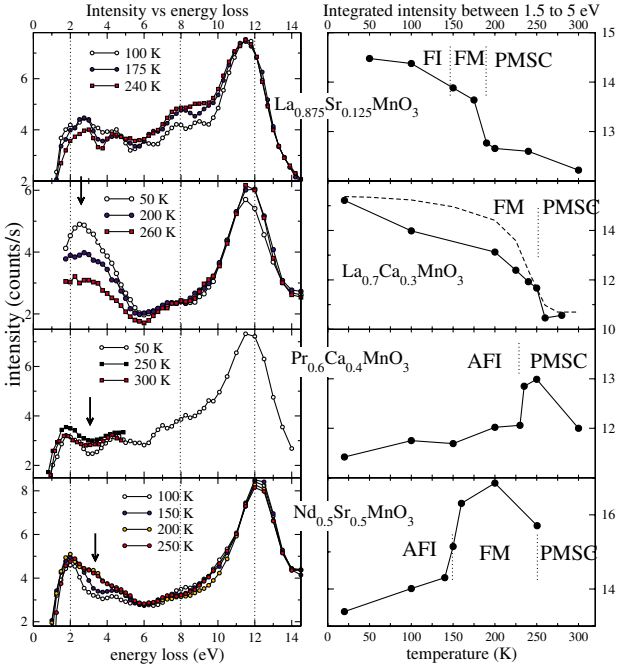

FIG. 2 (color online). (Left panels) Selected energy-loss spectra versus temperature after subtraction of the quasielastic line. The arrows indicate the region of maximum temperature dependence. (Right panels) Integrated spectral intensity between 1.5 and 5 eV. For LCMO.3, the increase is compared to the magnetization (dashed line, taken from Ref. [9]).

cross section and the magnetization is not linear (Fig. 2). Note that the large quasielastic scattering obscures the energy range below 1 eV where the closing of the gap associated with the onset of metallicity occurs.

In order to understand the dependence of the inelastic x-ray scattering on the magnetism, we calculated the electronic structure and the RIXS response function with time-dependent density functional theory using the local density approximation + Hubbard U (LDA + U) approximation. To make the calculations tractable, we consider the prototypical orbitally ordered insulator $LaMnO_3$. However, we believe the insights gained are generally applicable.

We begin by calculating the electronic structure of $LaMnO_3$ in a structure with the Jahn-Teller (JT) distorted octahedra (but without tilting), taking $U = 8$ eV and $J = 0.88$ eV [18]. We find a ground state with A-type antiferromagnetic order and an insulating gap (Fig. 3). The gap

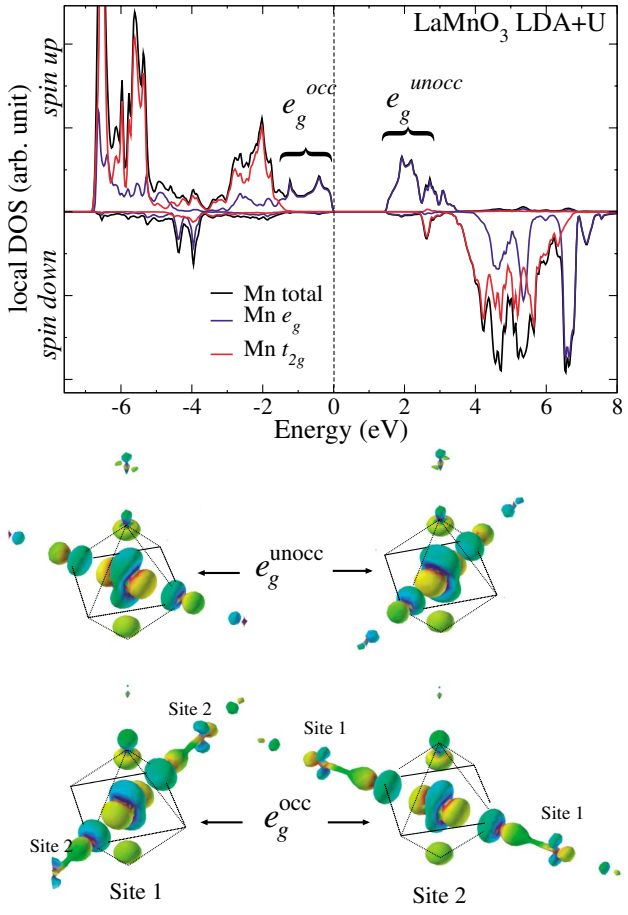

FIG. 3 (color). (Upper panel) Spin polarized Mn local density of states for $LaMnO_3$ calculated by LDA + U. (Lower panel) Isodensity plots of the Wannier functions for occupied and unoccupied e_g orbitals. Site 1 and site 2 are two first neighbor Mn in the a-b plane ($Pbnm$ setting) within the same reference frame: orbital ordering is obtained. The oxygen octahedra are depicted. Colors blue and green (red and yellow) represent higher and lower positive (negative) gradient of the wave functions.

results from a lifting of the degeneracy between the quarter-filled e_g states that accompanies the in-plane orbital ordering (which is driven mainly by the large on-site repulsion [18,19]). These findings are in good agreement with the actual ground state of $LaMnO_3$. The upper panel of Fig. 3 shows that the only states relevant to the low-energy excitations are the e_g states of the majority spin at the Mn sites. The real space distribution of these states is illustrated in the lower panel, in which the Wannier functions [19,20] of both the occupied (e_g^{occ}) and the unoccupied (e_g^{unocc}) states are shown for two neighboring sites. Remarkably, the calculations reproduce the staggered orbital ordering of the e_g^{occ} states, with a significant overlap with neighboring Mn sites mediated by hybridization with the O $2p$ states.

The mechanism for the observed temperature dependence of the RIXS spectra can be understood in the following way: In the small-q region, the low-energy features in the RIXS spectra are dominated by *intersite d-d* transitions between Mn atoms (mediated via the O-$2p$). Ignoring improbable spin-flip excitations, such intersite transitions can occur only between neighbors with the same spin alignment, since no states exist at low-energy in the opposite spin channel (upper panel, Fig. 3). This is illustrated schematically in Fig. 4(a). Thus the more pairs of ferromagnetically aligned neighbors in the system, the stronger the low-energy spectra will be, consistent with our experiments.

This picture was confirmed by calculations of the dielectric function, $\varepsilon(q, \omega)$, whose imaginary part reflects the spectrum of allowed transitions [Fig. 4(b)] [21,22]. The calculation was performed twice for the same JT-distorted, untilted structure: once for A-type AF magnetic ordering, and once for ferromagnetic ordering. The momentum transfer was taken to be similar to that of the experiments, after mapping back to the first Brillouin zone. The ferromagnetic dielectric function is doubled relative to the AF one [Fig. 4(b)], as is $S(q, \omega)$ at low energies (not shown). This enhancement results from the additional charge transfer along the c axis, via the apical O (Fig. 3), which is allowed for the ferromagnetic structure and suppressed for the A-type AF. This additional contribution is of similar size to that arising from transitions within the a-b plane because, despite the ferromagnetic correlations of the four Mn nearest neighbors in plane, only two contribute, due to the directional nature of the ordered orbitals, as illustrated by the Wannier functions (Fig. 3). In the actual doped systems, this difference may be reduced for various reasons, including changes in orbital ordering, degree of hybridization, the bandwidth of the e_g states, and screening due to metallization. However, the qualitative trend is expected to persist and explains the present results.

Our calculations further allow one to discuss the connection between the RIXS cross section and a calculable response function. Several authors have argued that for K-edge resonant IXS, the cross section is proportional to

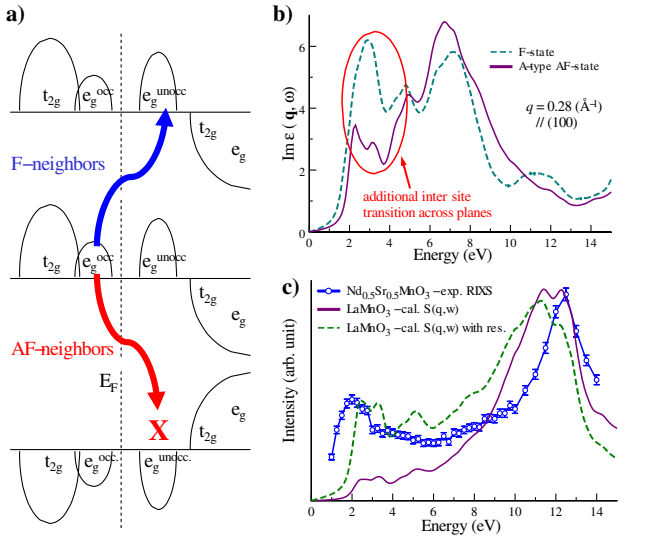

FIG. 4 (color online). (a) Schematic for the possible hopping between neighboring sites. For ferromagnetic neighbors, low-energy excitations are allowed (upper arrow). For antiferromagnetic neighbors, such excitations require an improbable spin flip and are suppressed (lower arrow). (b) Imaginary part of the dielectric function for two magnetic ground states of $LaMnO_3$. (c) Comparison between the RIXS spectra for the AFI NSMO.5 and the calculated $S(q, \omega)$ for AFI $LaMnO_3$, with and without the resonant factors (see text).

the nonresonant IXS cross section, $S(q, \omega) \propto \mathrm{Im}(\frac{-1}{\varepsilon})$ (the loss function) multiplied by a term accounting for the resonance [23–25]. In Fig. 4(c) we show a comparison between the NSMO.5 data (low temperature AFI) and the calculated $S(q, \omega)$ for $LaMnO_3$ (low temperature AFI), with or without the resonant factor: The weighted $S(q, \omega)$ resembles the data. Note that, because of their precise relationship, the RIXS and optical conductivity response functions can have different temperature behaviors. For instance, if $\mathrm{Im}(\varepsilon) = \sigma_{\mathrm{opt}}$ tends to zero, $S(q, \omega) \propto \sigma_{\mathrm{RIXS}}$ feels the pole and increases. Thus there is no inconsistency between the different temperature dependences observed in the optical spectra and the present data [14–16].

Before concluding, we briefly comment on the high-energy data. The 8 eV region has weaker and opposite temperature dependence to that of the low-energy region. In Fig. 3 (upper panel) and Fig. 4, we see that the 8 eV region corresponds to transitions from the majority states to the minority states of an AF neighbor. A decrease within a ferromagnetic phase is therefore consistent with our picture. As to the 12 eV feature, it was observed in $LaMnO_3$ with RIXS and was attributed to a transition involving Mn states [5]. However, no excitation is seen around 12 eV in the optical spectra of the manganites [10,26]. Also, as shown in Fig. 2, substituting the earth cations does not significantly change the position of this feature. Thus, it is clearly a feature of $S(q, \omega)$ [Fig. 4(c)] and our calculations indicate that it is more of a collective response of the system as a whole, i.e., a damped plasmon, as $|\varepsilon| \leq 1$.

Summarizing, we have measured temperature dependence in the RIXS spectra of several manganites up to 10 eV energy loss. In the lowest energy range, we find that the excitation spectrum does not depend on the presence or the absence of orbital order, but does reflect the magnetic order of the sample. We have presented the local density of states for $LaMnO_3$ and the Wannier functions for the e_g states and explain the magnetic order dependent features as arising from intersite $3d$-$3d$ excitations. We also show that the loss function, as calculated from LDA + U, satisfactorily accounts for the RIXS spectra, including both single particle excitations and collective modes. Finally, this work highlights the sensitivity of the RIXS technique to magnetic correlations in manganites in addition to the charge excitations.

We thank P. Abbamonte, V. Oudovenko, J. Rehr, J. van den Brink, and M. van Veenendaal for fruitful discussions. Use of APS was supported by the U.S. DOE, Office of Basic Energy Sciences, under Contract No. W-31-109-Eng-38. Brookhaven National Laboratory is supported under DOE Contract No. DE-AC02-98CH10886. Support from the NSF MRSEC Program, Grant No. DMR-0080008, and from the NSF Grant No. DMR-0093143 are also acknowledged.

[1] M. B. Salamon and M. Jaime, Rev. Mod. Phys. **73**, 583 (2001).
[2] E. Dagotto *et al.*, Phys. Rep. **344**, 1 (2001).
[3] C. C. Kao *et al.*, Phys. Rev. B **54**, 16 361 (1996).
[4] W. Schülke, J. Phys. Condens. Matter **13**, 7557 (2001).
[5] T. Inami *et al.*, Phys. Rev. B **67**, 045108 (2003).
[6] K. Ishii *et al.*, Phys. Rev. B **70**, 224437 (2004).
[7] S. Grenier *et al.*, Physica (Amsterdam) **345B**, 6 (2004).
[8] Y.-J. Kim *et al.*, Phys. Rev. Lett. **92**, 137402 (2004).
[9] J. W. Lynn *et al.*, Phys. Rev. Lett. **76**, 4046 (1996).
[10] Y. Okimoto *et al.*, Phys. Rev. B **55**, 4206 (1997).
[11] Y. Okimoto *et al.*, Phys. Rev. B **59**, 7401 (1999).
[12] J. H. Jung *et al.*, Phys. Rev. B **55**, 15 489 (1997).
[13] J. H. Jung *et al.*, Phys. Rev. B **62**, 481 (2000).
[14] M. Quijada *et al.*, Phys. Rev. B **58**, 16 093 (1998).
[15] N. N. Kovaleva *et al.*, Phys. Rev. Lett. **93**, 147204 (2004).
[16] K. Tobe *et al.*, Phys. Rev. B **64**, 184421 (2001).
[17] K. H. Ahn and A. J. Millis, Phys. Rev. B **61**, 13 545 (2000).
[18] V. I. Anisimov *et al.*, Phys. Rev. B **55**, 15 494 (1997).
[19] W. Yin *et al.* (unpublished).
[20] W. Ku *et al.*, Phys. Rev. Lett. **89**, 167204 (2002).
[21] W. Ku *et al.*, Phys. Rev. Lett. **88**, 057001 (2002).
[22] W. Ku *et al.* (unpublished).
[23] P. M. Platzman and E. D. Isaacs, Phys. Rev. B **57**, 11 107 (1998).
[24] P. Abbamonte *et al.*, Phys. Rev. Lett. **83**, 860 (1999).
[25] J. van den Brink and M. van Veenendaal, cond-mat/0311446.
[26] T.-h. Arima and Y. Tokura, J. Phys. Soc. Jpn. **64**, 2488 (1995).